

2005

Higher Twist Analysis of the Proton g_1 Structure Function

M. Osipenko

W. Melnitchouk

S. Simula

P. Bosted

V. Burkert

See next page for additional authors

Follow this and additional works at: https://digitalcommons.odu.edu/physics_fac_pubs



Part of the [Astrophysics and Astronomy Commons](#), [Elementary Particles and Fields and String Theory Commons](#), and the [Quantum Physics Commons](#)

Original Publication Citation

Osipenko, M., Melnitchouk, W., Simula, S., Bosted, P., Burkert, V., Christy, M. E., Griffioen, K., Keppel, C., & Kuhn, S. E. (2005). Higher twist analysis of the proton g_1 structure function. *Physics Letters B*, 609(3-4), 259-264. <https://doi.org/10.1016/j.physletb.2005.01.071>

This Article is brought to you for free and open access by the Physics at ODU Digital Commons. It has been accepted for inclusion in Physics Faculty Publications by an authorized administrator of ODU Digital Commons. For more information, please contact digitalcommons@odu.edu.

Authors

M. Osipenko, W. Melnitchouk, S. Simula, P. Bosted, V. Burkert, M. E. Christy, K. Griffioen, C. Keppel, and S. E. Kuhn



ELSEVIER

Available online at www.sciencedirect.com

SCIENCE @ DIRECT®

Physics Letters B 609 (2005) 259–264

PHYSICS LETTERS B

www.elsevier.com/locate/physletb

Higher twist analysis of the proton g_1 structure function

M. Osipenko ^a, W. Melnitchouk ^b, S. Simula ^c, P. Bosted ^b, V. Burkert ^b, M.E. Christy ^d,
K. Griffioen ^e, C. Keppel ^{b,d}, S.E. Kuhn ^f

^a INFN, Sezione di Genova, 16146 Genoa, Italy

^b Jefferson Lab, 12000 Jefferson Avenue, Newport News, VA 23606, USA

^c INFN, Sezione Roma III, 00146 Roma, Italy

^d Hampton University, Hampton, VA 23668, USA

^e College of William & Mary, Williamsburg, VA 23187, USA

^f Old Dominion University, Norfolk, VA 23529, USA

Received 23 November 2004; accepted 12 January 2005

Available online 2 February 2005

Editor: W. Haxton

Abstract

We perform a global analysis of all available spin-dependent proton structure function data, covering a large range of Q^2 , $1 \leq Q^2 \leq 30 \text{ GeV}^2$, and calculate the lowest moment of the g_1 structure function as a function of Q^2 . From the Q^2 dependence of the lowest moment we extract matrix elements of twist-4 operators, and determine the color electric and magnetic polarizabilities of the proton to be $\chi_E = 0.026 \pm 0.015(\text{stat}) \pm 0.021(\text{sys})$ and $\chi_B = -0.013 \mp 0.007(\text{stat}) \mp 0.012(\text{sys})$, respectively.

© 2005 Elsevier B.V. All rights reserved.

PACS: 12.38.Aw; 12.38.Qk; 13.60.Hb

Measurements of spin-dependent structure functions of the proton reveal fundamental information about the proton's quark and gluon structure. In the quark-parton model, the g_1 structure function is interpreted in terms of distributions of quarks carrying light-cone momentum fraction x , with spins aligned versus anti-aligned with that of the nucleon. The lowest moment, or integral over x , of g_1 also determines the total spin carried by quarks in the nucleon.

Although most structure function studies have focused on the scaling regime at high four-momentum transfer squared, Q^2 , the behavior of g_1 and its moments in the transition region at intermediate Q^2 ($\sim 1 \text{ GeV}^2$) can reveal rich information about the long-distance structure of the nucleon. One example of the complexity of this region is the transition from the Bjorken or Ellis–Jaffe sum rules at high Q^2 to the Gerasimov–Drell–Hearn sum rule at $Q^2 = 0$ [1].

Of particular importance in this region is the role of the nucleon resonances, and the interplay between resonant and scaling contributions. According to the

E-mail address: wmelnitc@jlab.org (W. Melnitchouk).

operator product expansion (OPE) in QCD, the appearance of scaling violations at low Q^2 is related to the size of higher twist corrections to moments of structure functions [2]. Higher twists are expressed as matrix elements of operators involving nonperturbative interactions between quarks and gluons. The study of higher twist corrections thus gives us direct insight into the nature of long-range quark–gluon correlations.

In this Letter we determine the size of the higher twist contributions to the lowest moment of the g_1 structure function of the proton. We analyze the entire set of available data from experiments at SLAC [3–6], CERN [7,8], DESY [9], and most recently Jefferson Lab [10], where high-precision data in the resonance region and at low and intermediate Q^2 have been taken. Combining the moment data from the various experiments is nontrivial, however, since different analyses typically make use of different assumptions about extrapolations into unmeasured regions of kinematics. In the present analysis, we therefore extract the structure function moment using a single set of inputs and assumptions for *all* the data.

The lowest (Cornwall–Norton) moment of the proton g_1 structure function is defined as

$$\Gamma_1(Q^2) = \int_0^1 dx g_1(x, Q^2). \quad (1)$$

The upper limit includes the proton elastic contribution at $x \equiv Q^2/2M\nu = 1$, where ν is the energy transfer, and M is the proton mass. The inclusion of the elastic component is essential if one wishes to use the OPE to study the evolution of the integral in the moderate Q^2 region [11].

From the OPE, at large Q^2 the moment Γ_1 can be expanded in powers of $1/Q^2$, with the expansion coefficients related to nucleon matrix elements of operators of a definite twist (defined as the dimension minus the spin of the operator). At high Q^2 the moment is dominated by the leading twist contribution, μ_2 , which is given in terms of matrix elements of the twist-2 axial vector current, $\bar{\psi}\gamma^\mu\gamma_5\psi$. This can be decomposed into flavor singlet and nonsinglet contributions as

$$\mu_2(Q^2) = C_s(Q^2) \frac{a_0^{\text{inv}}}{9} + C_{\text{ns}}(Q^2) \left(\frac{a_3}{12} + \frac{a_8}{36} \right), \quad (2)$$

where C_s and C_{ns} are the singlet and nonsinglet Wilson coefficients, respectively [12], which are calculated as a series in α_s . The triplet and octet axial charges, $a_3 = g_A = 1.267$ and $a_8 = 0.58$, are extracted from weak decay matrix elements. For the singlet axial charge, we work with the renormalization group invariant definition in the $\overline{\text{MS}}$ scheme, $a_0^{\text{inv}} = a_0$ ($Q^2 = \infty$), in which all of the Q^2 dependence is factorized into the Wilson coefficient C_s .

Considerable effort has been made over the past two decades in determining the singlet axial charge, which in the quark–parton model is identified with the total spin carried by quarks in the proton. In this work we focus instead on using the world’s data to extract the coefficient of the $1/Q^2$ subleading, twist-4 term, which contains information on quark–gluon correlations in the nucleon.

In addition to the twist-4 matrix element, the $1/Q^2$ term also contains so-called “kinematic” higher twists, associated with target mass corrections (which are formally twist-2), and the g_2 structure function, which is obtained from measurements with transversely polarized targets. One technique for removing these from the $1/Q^2$ correction is to work in terms of the Nachtmann moment [13],

$$M_1(Q^2) = \int_0^1 dx \frac{\xi^2}{x^2} \left\{ g_1(x, Q^2) \left(\frac{x}{\xi} - \frac{1}{9} \frac{M^2 x \xi}{Q^2} \right) - g_2(x, Q^2) \frac{4}{3} \frac{M^2 x^2}{Q^2} \right\}, \quad (3)$$

where $\xi = 2x/(1 + \sqrt{1 + 4M^2x^2/Q^2})$ is the Nachtmann scaling variable. The twist expansion of $M_1(Q^2)$ then yields

$$M_1(Q^2) = \mu_2(Q^2) + \frac{\mu_4(Q^2)}{Q^2} + \frac{\mu_6(Q^2)}{Q^4} + \dots, \quad (4)$$

where μ_2 is given in Eq. (2). The $1/Q^2$ correction in Eq. (4) exposes directly the “dynamical” twist-4 coefficient f_2 , since $\mu_4(Q^2) = 4f_2(Q^2)/9M^2$, where f_2 is given in terms of a mixed quark–gluon operator,

$$f_2(Q^2) M^2 S^\mu = \frac{1}{2} \sum_q e_q^2 \langle N | g \bar{\psi}_q \tilde{G}^{\mu\nu} \gamma_\nu \psi_q | N \rangle. \quad (5)$$

Here $\tilde{G}^{\mu\nu} = \frac{1}{2} \epsilon^{\mu\nu\alpha\beta} G_{\alpha\beta}$ is the dual of the gluon field strength tensor, S^μ is the proton spin vector, g is the strong coupling constant, and e_q is the quark charge.

Clearly the $1/Q^2$ term can be best determined in the intermediate Q^2 region, where Q^2 is neither so large as to completely suppress the higher twists, nor so small as to render the twist expansion unreliable. A meaningful analysis of data from different experiments further requires that the same set of inputs be used in the determination of g_1 , as well as g_2 .

In practice one must reconstruct g_1 from a combination of longitudinal (A_{\parallel}) and transverse (A_{\perp}) polarization asymmetries, together with the unpolarized F_1 structure function, and the ratio R of the longitudinal to transverse cross sections. We begin by collecting all available data on A_{\parallel} , as published in Refs. [3–10], and use the same inputs in the analysis of A_{\perp} , F_1 and R for all the data sets.

To provide a realistic description of A_{\perp} , or equivalently A_2 (which is given in terms of A_{\parallel} and A_{\perp} [5]), we consider both the resonance and nonresonant background contributions. For the background we use the (twist-2) Wandzura–Wilczek (WW) relation [14]. Inclusion of target mass corrections in the WW formula [14] enables this prescription to be used down to low Q^2 , where target mass corrections are known to be important [2]. In the resonance region, however, the WW approximation fails, and here alternative parameterizations are required. We calculate the resonance contribution from the electromagnetic helicity amplitudes $S_{1/2}(Q^2)$ and $A_{1/2}(Q^2)$ obtained in the constituent quark model [15], which includes 14 major resonances. The resonance contribution is then normalized to satisfy the Burkhardt–Cottingham sum rule [16]. The A_2 model is consistent with the available data [17,18], as well as with the model-independent Soffer bound [19].

For the ratio $R(x, Q^2)$ we use a new parameterization based on Rosenbluth-separated cross sections [20,21], which is adapted to the low- Q^2 and low- W^2 region, and smoothly interpolates to the earlier parameterization of the deep inelastic region from Ref. [22]. This parameterization uses all published data in the resonance region [23], as well as new data from Ref. [20].

The spin-averaged proton cross section is well determined in both the resonance and deep inelastic regions. At high Q^2 the effect of R is small and the differential cross section $d\sigma/d\Omega dE'$ is proportional to F_2 (or F_1). At moderate Q^2 , however, the extraction of F_1 and F_2 from the cross section requires knowledge

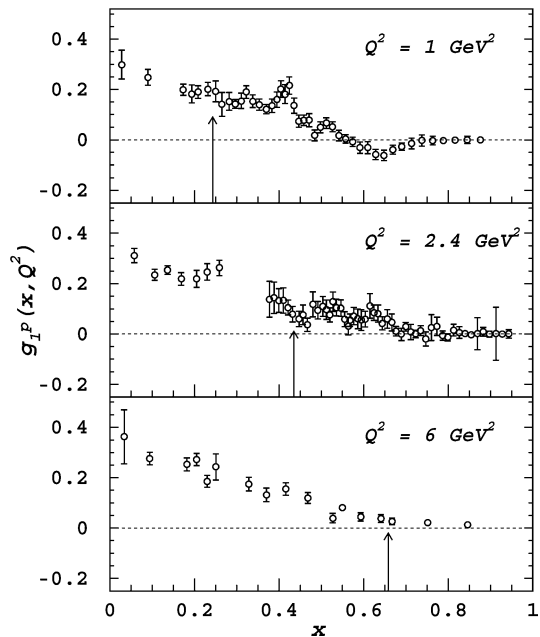


Fig. 1. Proton g_1 structure function at several different Q^2 values. The points represent reanalyzed experimental data obtained from the longitudinal asymmetry A_{\parallel} from Refs. [3–10] using the procedure described in the text. The vertical arrows indicate the boundary between the resonance (to the right of the arrow) and deep inelastic regions ($W = 2$ GeV).

of R . Using the parametrization of R from Ref. [20], we constructed a database of world data on F_1 from which values of F_1 corresponding to the measured A_{\parallel} kinematic points were obtained by interpolation. Most of the data points for A_{\parallel} have kinematically close sets of $d^2\sigma/d\Omega dE'$ points, which allows interpolation uncertainties to be minimized. Full details of the extraction of g_1 will be provided in a forthcoming publication [21].

The resulting g_1 structure function is illustrated in Fig. 1 as a function of x for several representative Q^2 values. The vertical arrows indicate the boundary between the resonance and deep inelastic regions at $W = 2$ GeV. At the lower Q^2 values, $Q^2 \sim 1$ GeV², a significant portion of the x range is in the resonance region (contributing $\sim 40\%$ of the magnitude of the lowest moment).

The first moment of g_1 is evaluated using the same method as in recent analyses of the unpolarized proton F_2 structure function moments [24,25]. This method is essentially independent of assumptions about the x

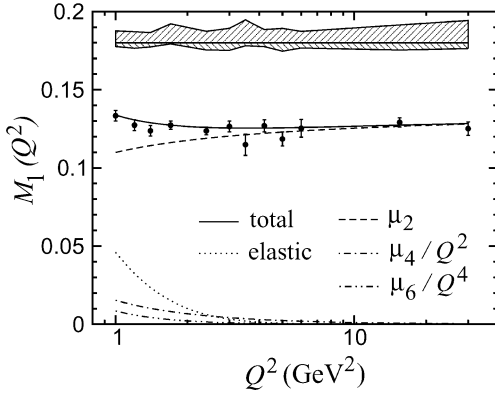


Fig. 2. Q^2 dependence of the Nachtmann moment $M_1(Q^2)$. The error bars are statistical, with the systematic errors indicated by the hashed areas (see text). The leading twist (dashed), $1/Q^2$ (dot-dashed), $1/Q^4$ (dot-dot-dashed) and elastic (dotted) contributions are shown separately. The solid curve is the sum of leading and higher twist terms.

dependence of the structure function when interpolating between data points, and is therefore well-suited for a study of Q^2 evolution of the moments. For the low- x extrapolation, beyond the region where data exist, we use the Regge model-inspired parametrization from Ref. [26]. To estimate the uncertainty associated with the low- x extrapolation, we also consider other parameterizations [27], and take the maximum difference between the respective low- x contributions as the error.

The resulting Nachtmann moment $M_1(Q^2)$ is shown in Fig. 2, where the error bars on the data points are statistical only. The systematic errors, some of which are correlated, are shown separately in the hashed areas above the data, and represent uncertainties from the low- x extrapolation (lower hashed area), and the experimental systematic errors together with those from A_2 , R and an estimated 5% uncertainty on the elastic contribution (upper hashed area). The g_2 contribution to M_1 is obtained from A_{\parallel} , A_{\perp} , and F_1 , as determined from the present analysis (see Ref. [21] for details).

The fit to the total moment $M_1(Q^2)$ uses three parameters, a_0^{inv} , f_2 (or μ_4) and μ_6 , with the nonsinglet axial charges (g_A and a_8) as inputs. For the leading twist contribution we use a next-to-leading order approximation for the Wilson coefficients and the two-loop expression for α_s , which at $Q^2 = 1 \text{ GeV}^2$ corresponds to $\alpha_s^{\text{NLO}} = 0.45 \pm 0.05$ in the $\overline{\text{MS}}$ scheme.

In fitting the parameters, we have considered both multiparameter (simultaneous) fits and sequential fits, in which the leading twist term a_0^{inv} is first fitted to the high- Q^2 data, and then the higher twist terms are extracted. While both methods should in principle yield the same results when the experimental errors are small, in practice the multiparameter fit may not be the most suitable choice when emphasizing the high-precision low- Q^2 data. The multiparameter fit is most effective when the errors on the data are similar across the entire Q^2 range, and the number of points in the region which determines the leading twist contribution ($Q^2 \gtrsim 5 \text{ GeV}^2$) is similar to that which constrains the higher twists ($Q^2 \lesssim 5 \text{ GeV}^2$).

Assuming the data at high Q^2 are saturated by the twist-2 term alone, the fit to the $Q^2 > 5 \text{ GeV}^2$ data determines the singlet axial charge to be

$$a_0^{\text{inv}} = 0.145 \pm 0.018(\text{stat}) \pm 0.103(\text{sys}) \pm 0.041(\text{low } x) \pm_{0.010}^{0.006}(\alpha_s), \quad (6)$$

where the first and second errors are statistical and systematic, the third comes from the $x \rightarrow 0$ extrapolation, and the last is due to the uncertainty in α_s . We have considered the sensitivity of the results to the value of Q^2 used to constrain the leading twist term. We find that a_0^{inv} converges to the above value for $Q^2 \gtrsim 3\text{--}4 \text{ GeV}^2$. Fitting the $Q^2 > 10 \text{ GeV}^2$ data would lead to practically the same values of a_0^{inv} , but with a slightly larger error bar.

Having determined the twist-2 term from the high- Q^2 data, we now extract the $1/Q^2$ and $1/Q^4$ coefficients from the $1 \leq Q^2 \leq 5 \text{ GeV}^2$ data, fixing a_0^{inv} to the above value, but allowing it to vary within its statistical errors. For the twist-4 coefficient we find

$$f_2 = 0.039 \pm 0.022(\text{stat}) \pm_{0.018}^{0.000}(\text{sys}) \pm 0.030(\text{low } x) \pm_{0.011}^{0.007}(\alpha_s), \quad (7)$$

normalized at a scale $Q^2 = 1 \text{ GeV}^2$ (the Q^2 evolution of f_2 is implemented using the one-loop anomalous dimensions calculated in Ref. [28]). The systematic uncertainty on f_2 is determined by refitting the M_1 data shifted up or down by the M_1 systematic uncertainty shown in Fig. 2 (upper hashed area). The low- x extrapolation uncertainty is determined by fitting the M_1 values shifted by the maximum difference between the $x \rightarrow 0$ contributions calculated with the parameterizations from Refs. [26,27] (lower hashed area in

Fig. 2). The relative contribution from the low- x extrapolation to the asymptotic value of M_1 is $\approx 7\%$ and 15% at $Q^2 = 1$ and 3 GeV^2 , respectively. However, because the $x \rightarrow 0$ extrapolation affects more the overall magnitude of M_1 rather than its Q^2 dependence, the effect on f_2 is relatively small.

For the $1/Q^4$ term, the best fit to the $1 \leq Q^2 \leq 5 \text{ GeV}^2$ data yields $\mu_6/M^4 = 0.011 \pm 0.013(\text{stat}) \pm 0.010(\text{sys}) \pm 0.011(\text{low } x) \pm 0.000(\alpha_s)$, with the errors determined as for f_2 . Within the present level of accuracy the Q^2 evolution of the coefficient μ_6 can be neglected. The $1/Q^2$ and $1/Q^4$ contributions to M_1 are illustrated in Fig. 2. For comparison, the elastic contribution is also shown, as is the sum of the leading plus higher twist contributions. Since one is fitting M_1 in a relatively low Q^2 region, one may ask whether still higher-order corrections could be significant beyond those considered in Eq. (4). Adding a phenomenological μ_8/Q^6 term to the $Q^2 > 1 \text{ GeV}^2$ fit, and fixing the other parameters to their quoted values, gives a coefficient $\mu_8/M^6 = -0.004 \pm 0.004$ which is consistent with zero. To determine μ_8 more precisely one needs to go below $Q^2 \sim 1 \text{ GeV}^2$, however, it is not clear that the twist expansion is convergent at such low Q^2 .

Simply fitting the entire $1 < Q^2 < 30 \text{ GeV}^2$ data set using a 3-parameter fit, the value of the singlet charge would be essentially unchanged ($a_0^{\text{inv}} = 0.145 \pm 0.023(\text{stat})$), while the twist-4 coefficient would be slightly smaller, $f_2 = 0.016 \pm 0.039(\text{stat})$, but compatible with the above result (7) within uncertainties (with similar systematic errors as in Eqs. (6) and (7)).

In earlier phenomenological analyses [29,30] larger values of f_2 were obtained. Using the SLAC-E143 data [5], Ref. [29] found $f_2 = 0.10 \pm 0.05$, while Ref. [30] used in addition HERMES [9] and CLAS [10] data to extract a value $f_2 = 0.15\text{--}0.18$. In both cases, however, the $1/Q^4$ corrections in Eq. (4) were not included, which we find important even for $Q^2 \sim 1 \text{ GeV}^2$. This is particularly relevant for the analysis in Ref. [30], which assumes that the higher twists are dominated by the $1/Q^2$ term already at $Q^2 \sim 0.5 \text{ GeV}^2$. If one were to redo the present analysis with a 1-parameter fit as in Refs. [29,30], the statistical error on f_2^p from the $Q^2 > 1 \text{ GeV}^2$ data would be ~ 0.005 , which is 4–5 times smaller than that in the 2-parameter fit, and gives a 2–3 smaller combined statistical and systematic uncertainty than in Ref. [29].

The result of the present work (7) therefore represents a significant improvement over the earlier analyses.

From the extracted f_2 values one can calculate the contribution of the collective color electric and magnetic fields to the spin of the proton. These are given by [31,32]

$$\chi_E = \frac{2}{3}(2d_2 + f_2), \quad (8)$$

$$\chi_B = \frac{1}{3}(4d_2 - f_2), \quad (9)$$

where d_2 is given by the matrix element of the twist-3 operator $\bar{\psi}(\tilde{G}^{\mu\nu}\gamma^\alpha + \tilde{G}^{\mu\alpha}\gamma^\nu)\psi$, and can be extracted from the second moments of g_1 and g_2 ,

$$d_2(Q^2) = \int_0^1 dx x^2 [2g_1(x, Q^2) + 3g_2(x, Q^2)], \quad (10)$$

as determined from the present analysis. We find, however, that its leading twist component is negligible, and consistent with zero.

Combining the extracted f_2 and d_2 values obtained from the global analysis, we find

$$\chi_E = 0.026 \pm 0.015(\text{stat}) \pm 0.021(\text{sys}), \quad (11)$$

$$\chi_B = -0.013 \mp 0.007(\text{stat}) \mp 0.010(\text{sys}), \quad (12)$$

where the low- x extrapolation and α_s uncertainties have been folded into the total systematic error. Since the color polarizabilities are dominated by f_2 , the sign of the color electric polarizability is positive, while that of the color magnetic polarizability is negative. The upper limit on f_2 in Eq. (7) thus yields non-zero values for χ_E and χ_B , while the lower limit gives values which are close to zero.

These results can be compared to model calculations. QCD sum rules generally predict negative values for the electric polarizabilities, and slightly positive values for the magnetic ones [31,33], $\chi_E^{\text{sum rule}} \approx -(0.03\text{--}0.04)$ and $\chi_B^{\text{sum rule}} \approx 0.01\text{--}0.02$, in contrast to the results in Eqs. (11) and (12). Similar results are found in the calculations based on the instanton vacuum model [34], $\chi_E^{\text{instanton}} \approx -0.03$ and $\chi_B^{\text{instanton}} \approx 0.015$. The MIT bag model on the other hand gives [11] $\chi_E^{\text{bag}} \approx 0.03\text{--}0.05$ and $\chi_B^{\text{bag}} \approx 0.00\text{--}0.02$, which is consistent with our findings.

More precise measurements of the structure functions at $Q^2 \approx 1\text{--}10 \text{ GeV}^2$, with smaller statistical and

systematic errors, would reduce the uncertainty in the extracted higher twist coefficients, as would better knowledge of α_s at the relatively low Q^2 values discussed here. The present findings suggest that higher twists in the lowest moment of the proton g_1 structure function are small and consistent with zero for $Q^2 \gtrsim 2\text{--}3 \text{ GeV}^2$ (see also Refs. [26,29,35,36]), which demonstrates, perhaps surprisingly, the usefulness of the OPE formalism at these rather low Q^2 values. Higher twists are expected to play a greater role in higher moments, which emphasize more the large- x region and receive larger resonance contributions at the same Q^2 [21]. Better determination of the g_2 structure function at moderate and high Q^2 is also vital for the determination of the d_2 matrix element, as well as of the g_1 structure function itself.

Acknowledgements

We would like to thank G. Ricco for helpful contributions. This work was supported in part by the US Department of Energy contract DE-AC05-84ER40150, under which the Southeastern Universities Research Association operates the Thomas Jefferson National Accelerator Facility, by DOE grants DE-FG02-96ER40960 (Old Dominion U.) and DE-FG02-96ER41003 (College of William and Mary), and by NSF grant 0099540 (Hampton U.).

References

- [1] M. Anselmino, B.L. Ioffe, E. Leader, *Yad. Fiz.* 49 (1989) 214 (in Russian);
V.D. Burkert, B.L. Ioffe, *Phys. Lett. B* 296 (1992) 223;
V.D. Burkert, B.L. Ioffe, *J. Exp. Theor. Phys.* 78 (1994) 619;
D. Drechsel, *Prog. Part. Nucl. Phys.* 34 (1995) 181.
- [2] A. De Rujula, et al., *Ann. Phys.* 103 (1977) 315.
- [3] M.J. Alguard, et al., *Phys. Rev. Lett.* 37 (1976) 1261;
M.J. Alguard, et al., *Phys. Rev. Lett.* 41 (1978) 70.
- [4] G. Baum, et al., *Phys. Rev. Lett.* 45 (1980) 2000.
- [5] K. Abe, et al., *Phys. Rev. D* 58 (1998) 112003.
- [6] P.L. Anthony, et al., *Phys. Lett. B* 493 (2000) 19.
- [7] J. Ashman, et al., *Nucl. Phys. B* 328 (1989) 1.
- [8] B. Adeva, et al., *Phys. Rev. D* 58 (1998) 112001;
B. Adeva, et al., *Phys. Rev. D* 60 (1999) 072004;
B. Adeva, et al., *Phys. Rev. D* 62 (2000) 079902, Erratum.
- [9] A. Airapetian, et al., *Phys. Lett. B* 442 (1998) 484.
- [10] R. Fatemi, et al., *Phys. Rev. Lett.* 91 (2003) 222002.
- [11] X. Ji, P. Unrau, *Phys. Lett. B* 333 (1994) 228.
- [12] S.A. Larin, T. van Ritbergen, J.A.M. Vermaseren, *Phys. Lett. B* 404 (1997) 153.
- [13] S. Wandzura, *Nucl. Phys. B* 122 (1977) 412;
S. Matsuda, T. Uematsu, *Nucl. Phys. B* 168 (1980) 181.
- [14] S. Wandzura, F. Wilczek, *Phys. Lett. B* 72 (1977) 195.
- [15] M. Ferraris, et al., *Phys. Lett. B* 364 (1995) 231.
- [16] H. Burkhardt, W.N. Cottingham, *Ann. Phys.* 56 (1970) 453.
- [17] P.L. Anthony, et al., *Phys. Lett. B* 553 (2003) 18.
- [18] P.L. Anthony, et al., *Phys. Lett. B* 458 (1999) 529;
K. Abe, et al., *Phys. Rev. Lett.* 76 (1996) 587.
- [19] J. Soffer, O.V. Teryaev, *Phys. Lett. B* 490 (2000) 106.
- [20] Y. Liang, et al., E94-110 Collaboration, *nucl-ex/0410027*.
- [21] M. Osipenko, et al., in preparation.
- [22] K. Abe, et al., *Phys. Lett. B* 452 (1999) 194.
- [23] J. Drees, et al., *Z. Phys. C* 7 (1981) 183;
K. Batzner, Ph.D. Thesis, 1972;
D. Baran, et al., *Phys. Rev. Lett.* 61 (1988) 400.
- [24] M. Osipenko, et al., *Phys. Rev. D* 67 (2003) 092001.
- [25] C.S. Armstrong, et al., *Phys. Rev. D* 63 (2001) 094008.
- [26] S. Simula, et al., *Phys. Rev. D* 65 (2002) 034017.
- [27] M. Glück, et al., *Phys. Rev. D* 63 (2001) 094005;
D. de Florian, R. Sassot, *Phys. Rev. D* 62 (2000) 094025.
- [28] E.V. Shuryak, A.I. Vainshtein, *Nucl. Phys. B* 201 (1982) 141;
H. Kawamura, et al., *Mod. Phys. Lett. A* 12 (1997) 135.
- [29] X. Ji, W. Melnitchouk, *Phys. Rev. D* 56 (1997) 1.
- [30] C.W. Kao, et al., *Phys. Rev. D* 69 (2004) 056004.
- [31] E. Stein, et al., *Phys. Lett. B* 353 (1995) 107.
- [32] X. Ji, in: *Proceedings of the 7th International Conference on the Structure of Baryons*, Santa Fe, NM, 1995, *hep-ph/9510362*.
- [33] I.I. Balitsky, V.M. Braun, A.V. Kolisnichenko, *JETP Lett.* 50 (1989) 61;
I.I. Balitsky, V.M. Braun, A.V. Kolisnichenko, *Phys. Lett. B* 242 (1990) 245;
I.I. Balitsky, V.M. Braun, A.V. Kolisnichenko, *Phys. Lett. B* 318 (1993) 648, Erratum.
- [34] N.Y. Lee, et al., *Phys. Rev. D* 65 (2002) 054008.
- [35] A. Airapetian, et al., *Phys. Rev. Lett.* 90 (2003) 092002.
- [36] N. Bianchi, A. Fantoni, S. Liuti, *Phys. Rev. D* 69 (2004) 014505.